Self validation of radiance measurements from the CERES (TRMM) instrument

Jack Paden[a], Dhirendra K. Pandey[a], Robert B. Lee III[b], and Kory J. Priestley[b]

[a]Science Applications International Corporation, One Enterprise Parkway, Suite 300, Hampton, VA 23666-5845

[b]Atmospheric Sciences Competency, NASA Langley Research Center, M.S. 420, Hampton, VA 23681-0001

ABSTRACT

Eight continuous months of earth-nadir-viewing radiance measurements from the 3-channel Tropical Rainfall Measuring Mission (TRMM,) Clouds and the Earth's Radiant Energy System (CERES) scanning radiometric measurement instrument, have been analyzed. While previous remote sensing satellites, such as the Earth Radiation Budget Experiment (ERBE) covered all subsets of the broadband radiance spectrum (total, longwave and shortwave.) CERES has two subset channels (window and shortwave) which do not give continuous frequency coverage over the total band. Previous experience with ERBE indicated the need for us to model the "equivalent" daytime longwave radiance using a window channel regression, which will allow us to validate the performance of the instrument using a three-channel inter-comparison. Limiting our consideration to the fixed azimuth plane, cross-track, scanning mode (FAPS), each nadir-viewing measurement was averaged into three subjective categories called daytime, nighttime, and twilight. Daytime was defined as any measurement taken when the solar zenith angle (SZA) was less than 90°; nighttime was taken to be any measurement where the SZA was greater than 117°; and twilight was everything else. Our analysis indicates that there are only two distinct categories of nadir-view data; daytime, and non-daytime (i.e., the union of the nighttime and twilight sets); and that the CERES longwave radiance is predictable to an accuracy of 1%, based on the SZA, and window channel measurements.

Keywords: remote sensing, validation, earth radiation budget, ERBE, CERES, TRMM

1. INTRODUCTION

Barkstrom[1] described the instruments used in the pioneering efforts to measure the Earth's outgoing longwave radiation using remote sensing satellites. Wielicki, et al.[2], described the CERES Instrument as part of the Earth Observing System (EOS) Experiment. The CERES instrument, sensors, and the Radiometric Calibration Facility (RCF) were described by Lee, et al.[3] The CERES instrument's three remote sensing thermistor-bolometer detectors were designed to detect radiation for the "total" spectrum from 0.3 to more than 100 μm; for the water-vapor "window" spectrum from 8 to 12 μm; and for the "shortwave" spectrum from 0.3 to 5 μm.

2. THE HARDWARE

The first instrument (the Proto-flight Model, or PFM) in the Clouds and the Earth's Radiant Energy System (CERES) program was launched as a flight-of-opportunity aboard the Tropical Rainfall Measuring Mission (TRMM) platform on 27 November 1997 from the Tanegashima Island Space Center complex in Japan. Other instruments aboard the TRMM platform were the TRMM Microwave Imager (TMI,) the Visible and InfraRed Sensor (VIRS,) the Lightning Imaging Sensor (LIS,) and a precipitation radar (PR). Due to the nature of the TRMM's primary mission (i.e., sampling tropical rainfall,) the orbital parameters of the TRMM vary significantly from those of all three ERBE platforms. The 350 kilometer altitude of the TRMM is about half of that for the Earth Radiation Budget Satellite (ERBS,) and one-third of that for ERBE instruments carried on the NOAA-9 and NOAA-10 platforms. The orbit of the TRMM platform is restricted to the ±35° latitude (tropical) region, which is considerably less than the ERBS ±57° latitude (temperate) region, and much less than the polar orbits of NOAA-9 and NOAA-10. In contrast to previous ERBE remote sensing earth radiation platforms, the window and shortwave channels (i.e., the subordinate detectors) on CERES do not provide broadband coverage across the total spectrum. This situation creates a problem in terms of validating the measurements obtained from the detectors, because one can no longer add the longwave and the shortwave components to determine the total. Our goal then is to provide a proxy for the longwave component which will allow us to predict either the total or the shortwave component, in the absence of either.

3. THE DATA

During the first 8 months of on-orbit operation, the PFM instrument was used to acquire data in three modes of operation called cross-track, along-track (which are sometimes jointly referred to as fixed azimuth plane scanning or FAPS,) and biaxial (a rotating azimuth plane mode referred to as RAPS.) For the 8-month period, there were 169 days of FAPS (crosstrack) radiance measurements, 69 days of RAPS (biaxial) measurements, and 9 days of alongtrack measurements. Data were not available for 2 days (7 & 8 January 1998) when the sensors were calibrated for zero radiance offset measurements using various elevation and azimuth observation angles. As one would expect because of this sampling, the FAPS mode was dominant in the combined set. Time series plots for all CERES daylight measurements for the entire 8-month period from 1 January 1998 to 31 August 1998 are shown in Figures 1 through 3; for nighttime measurements in Figures 4 through 6; and for twilight measurements in Figures 7 through 9. This is shown for information only, as our primary goal in this analysis is to develop a time-independent relationship between the window channel and the *derived* longwave radiance. Of particular interest is the stability demonstrated by the shortwave channel at night, shown in Figure 6.

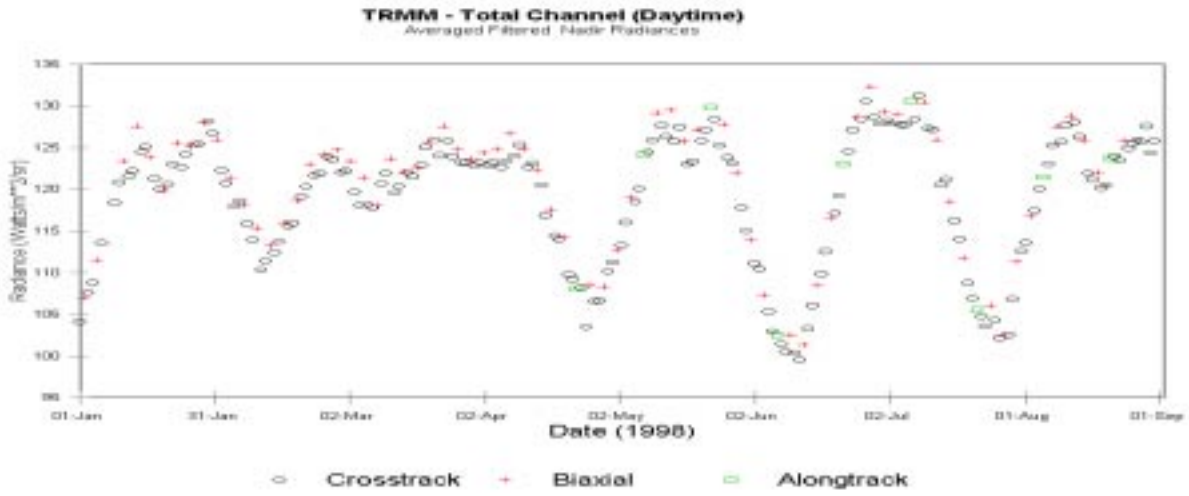

Figure 1. Daytime Total Channel - All modes (January - August 1998)

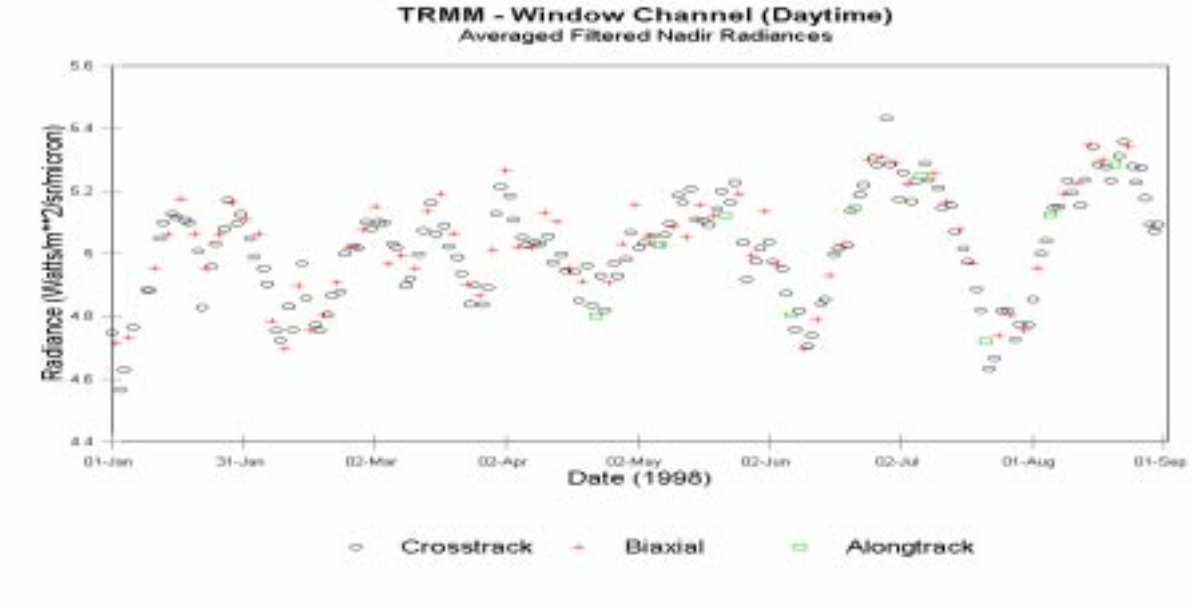

Figure 2. Daytime Window Channel - All modes (January - August 1998)

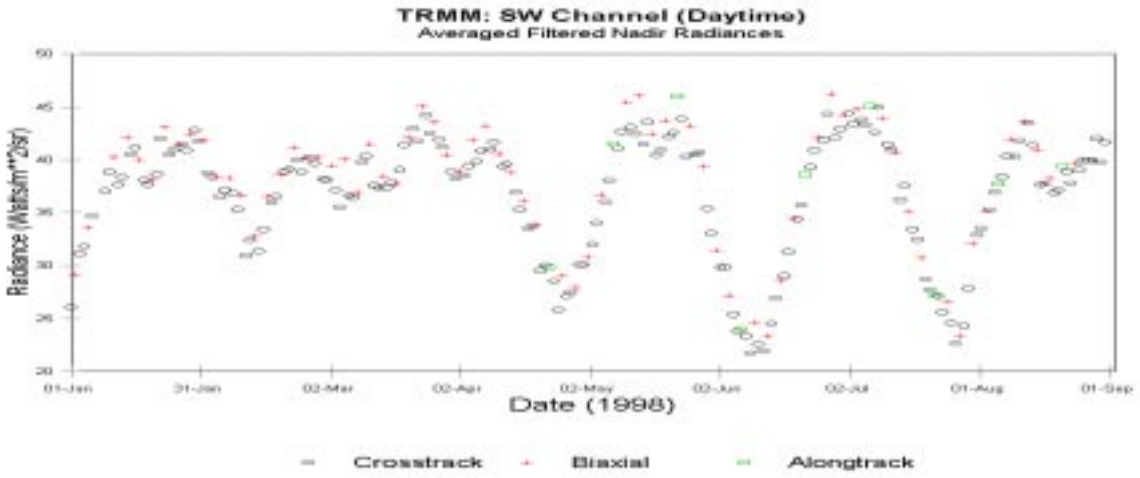

Figure 3. Daytime Shortwave Channel - All modes (January - August 1998)

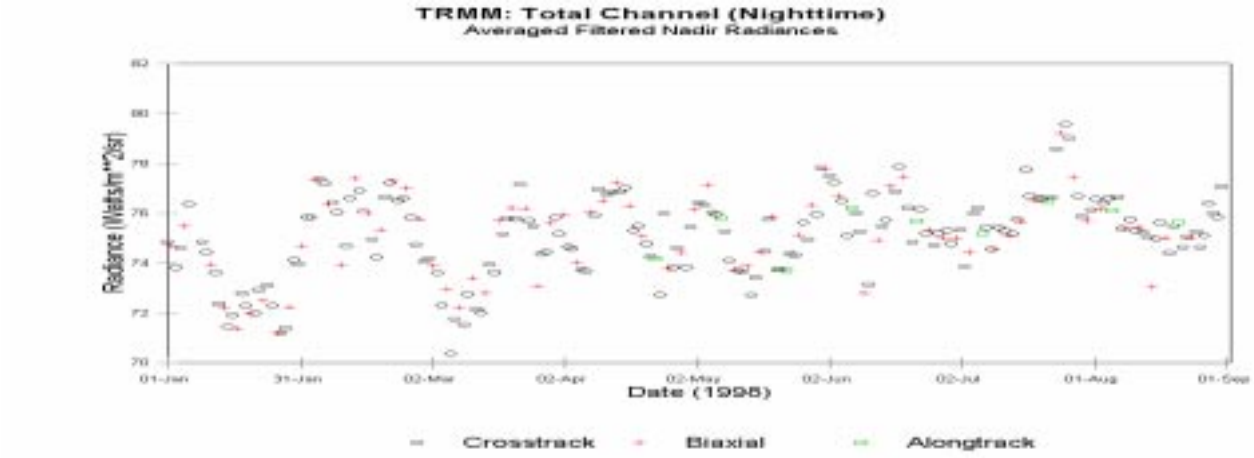

Figure 4. Nighttime Total Channel - All modes (January - August 1998)

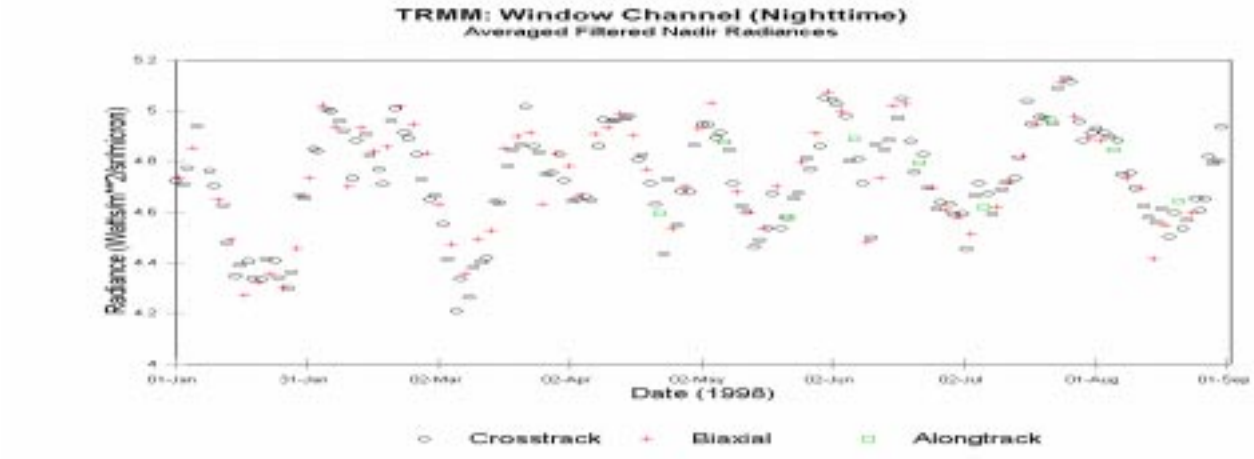

Figure 5. Nighttime Window Channel - All modes (January - August 1998)

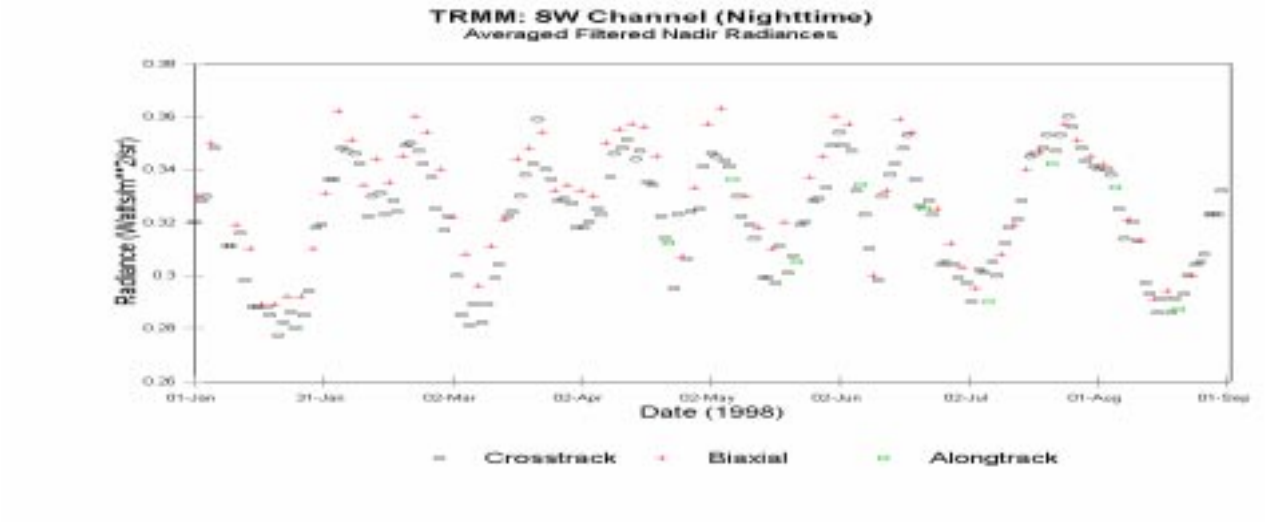

Figure 6. Nighttime Shortwave Channel - All modes (January - August 1998)

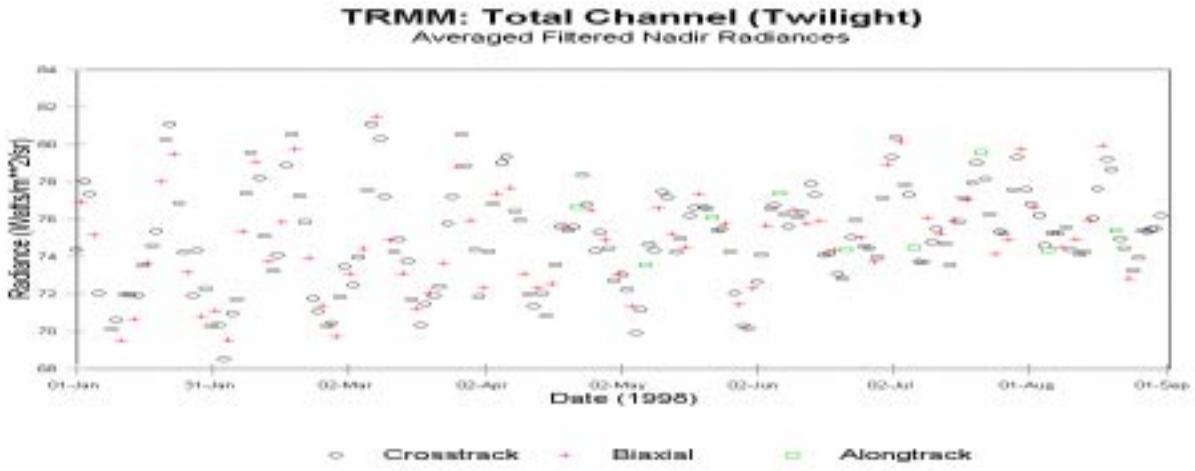

Figure 7. Twilight Total Channel - All modes (January - August 1998)

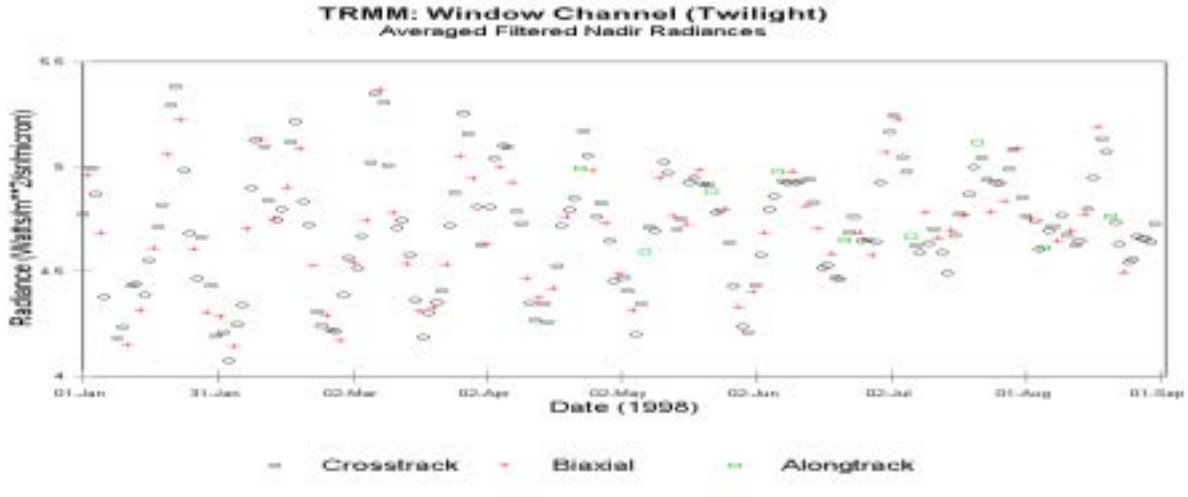

Figure 8. Twilight Window Channel - All modes (January - August 1998)

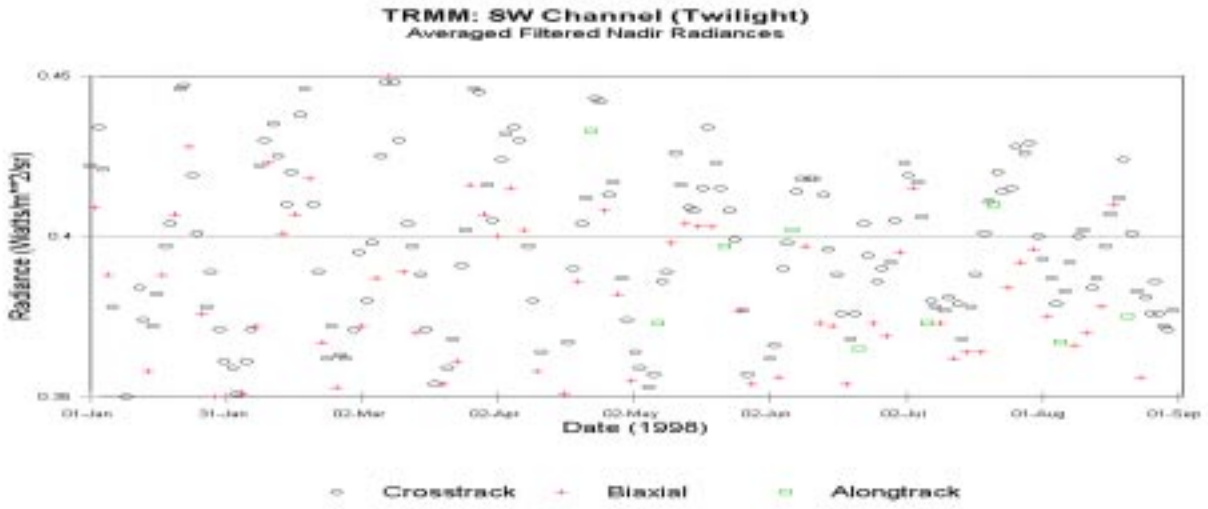

Figure 9. Twilight Shortwave Channel - All modes (January - August 1998)

The data which are analyzed in this paper are all from the FAPS, cross-track mode of operation which represents approximately 68% of the TRMM/CERES recorded data for this period. Our discussion is limited to this 8 month period because of CERES on-board power supply problems which occurred during August 1998. To date, the CERES/TRMM instrument continues to function, and the quality of the acquired data does not appear to be affected by the problem. Currently the instrument is being operated in a limited fashion, to prevent the power supply from failing[4], and possibly affecting the other experiments aboard the TRMM platform. The CERES PFM is still used to scan the earth during special field missions such as the Nauru exercise; and to conduct inflight sensor calibrations. The PFM instrument is scheduled to return to fully operational status upon launch of the EOS-AM platform in 1999.

4. THE PROCESSING

The CERES instrument data acquisition rate is 100 samples per second. The CERES data record is 6.6 seconds in length, and therefore there are 660 samples in a CERES record. During a 6.6 second scan, in normal scan mode, the CERES detectors scan the surface of the earth twice, and therefore there are exactly two opportunities for nadir-viewing earth samples. In a 24-hour day, the CERES instrument will complete 13091 scans. There are thus a potential 26182 nadir-viewing samples per day, per channel.

For the purposes of this analysis we have segregated all of the nadir-viewing samples of the PFM for each day, and taken the mean value of these measurements as representing the average value for that day. The data was then further segregated into three separate data sets which we refer to as daytime, twilight, and nighttime. To delineate these categories, we used the solar zenith angle (or SZA: the angle between the satellite and the sun, as seen from the center of the earth) to define daytime as any sample where the SZA $\leq$ 90°. Twilight was taken as any sample acquired when 117° > SZA > 90°; and nighttime was defined as any sample taken when the SZA $\geq$ 117°. The 117° limit was used in the ERBE program to represent the mean value for total solar darkness at all sub-satellite points. For the TRMM platform the limiting angle is approximately 109°. In order to allow future comparisons of ERBE and CERES data, we defined a surrogate longwave measurement (which we call derived longwave) for the CERES as being the difference between the total and shortwave measurements. The same method was used on the ERBE experiment for the non-scanner instrument, which had only total and shortwave detectors, while the scanning instrument directly measured the longwave component. It was then possible to inter-compare the ERBE measurements from the scanning and the non-scanning instruments which were mounted on the same platform. Note that the CERES total and shortwave channels, and thus the derived longwave, were converted into the same units, (watts/meter^2/steradian), whereas the window channel is measured in units of watts/meter^2/steradian/micron to facilitate direct inter-comparison with MODIS measurements.

5. THE ANALYSIS

For the purposes of this analysis, the daytime, twilight, and nighttime data sets were loaded into a spreadsheet (in this case, Corel Quattro Pro Version 7.0.2.14) for analysis. We then calculated the “derived longwave” values as the difference between the total and the shortwave channels for each measurement. Linear regression of the derived long-

wave versus the window channel measurement for the daytime, nighttime, and twilight data sets are graphically displayed in Figures 10 through 12, respectively. The data are shown, along with the linear regression fit to the data, and its equation.

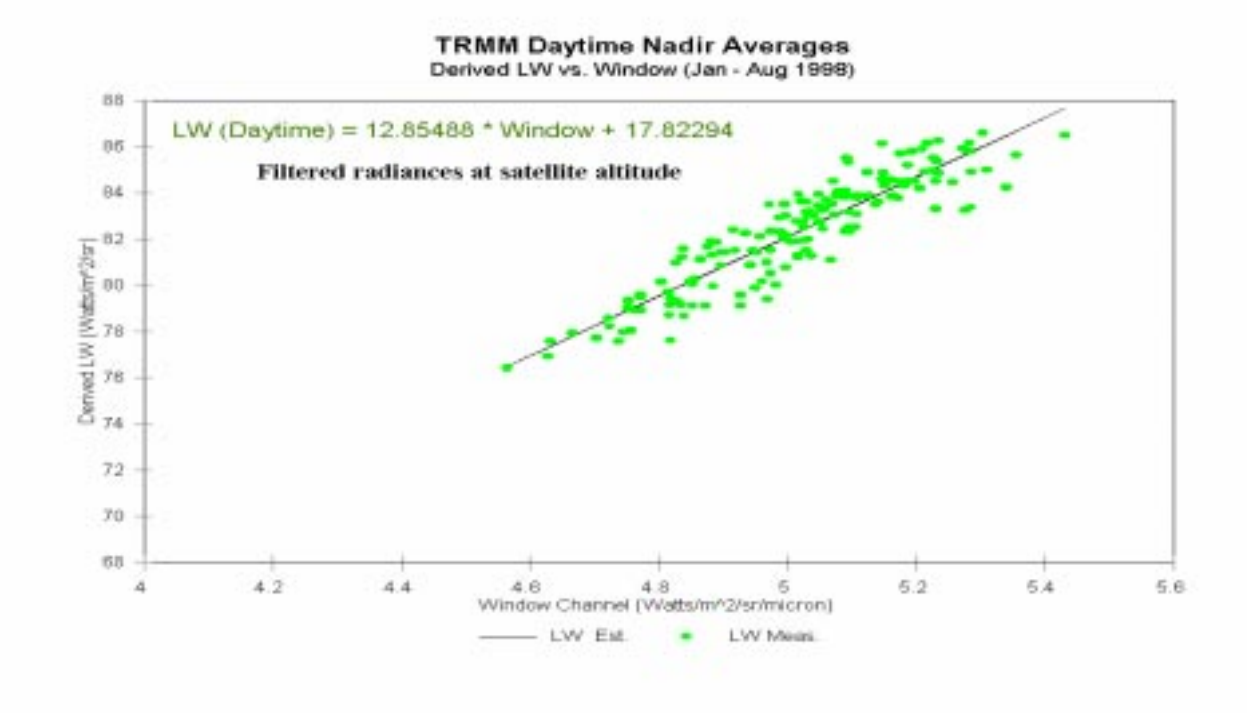

Figure 10. Daytime: Estimated LW vs. Window Channel

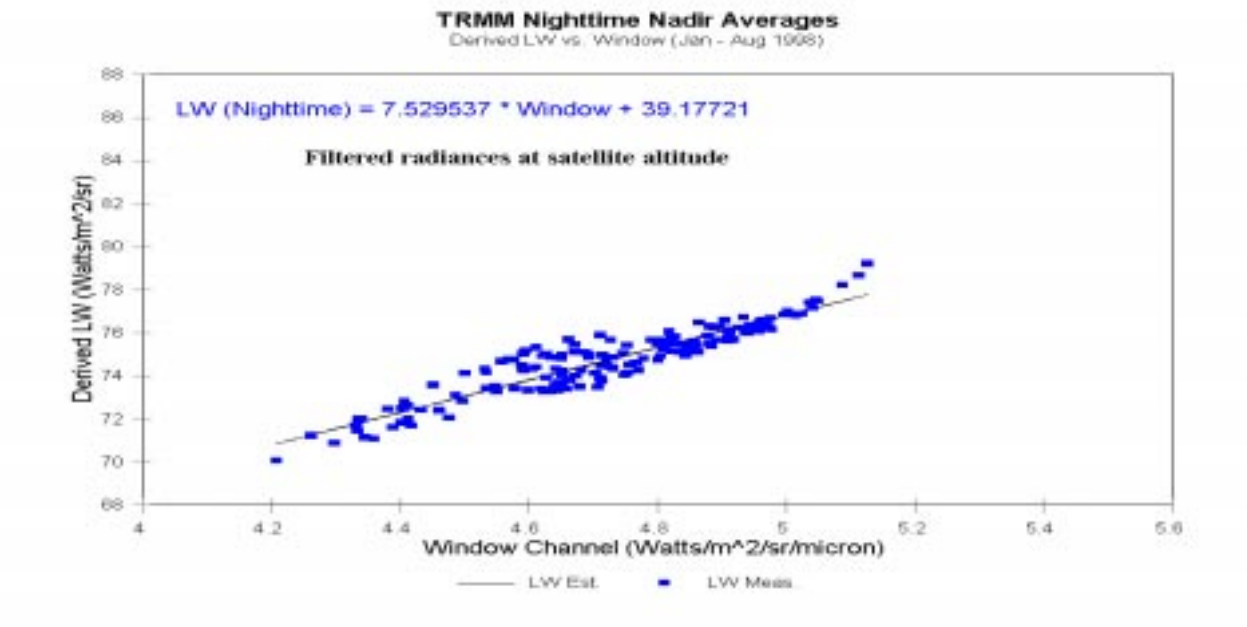

Figure 11. Nighttime: Estimated LW vs. Window Channel

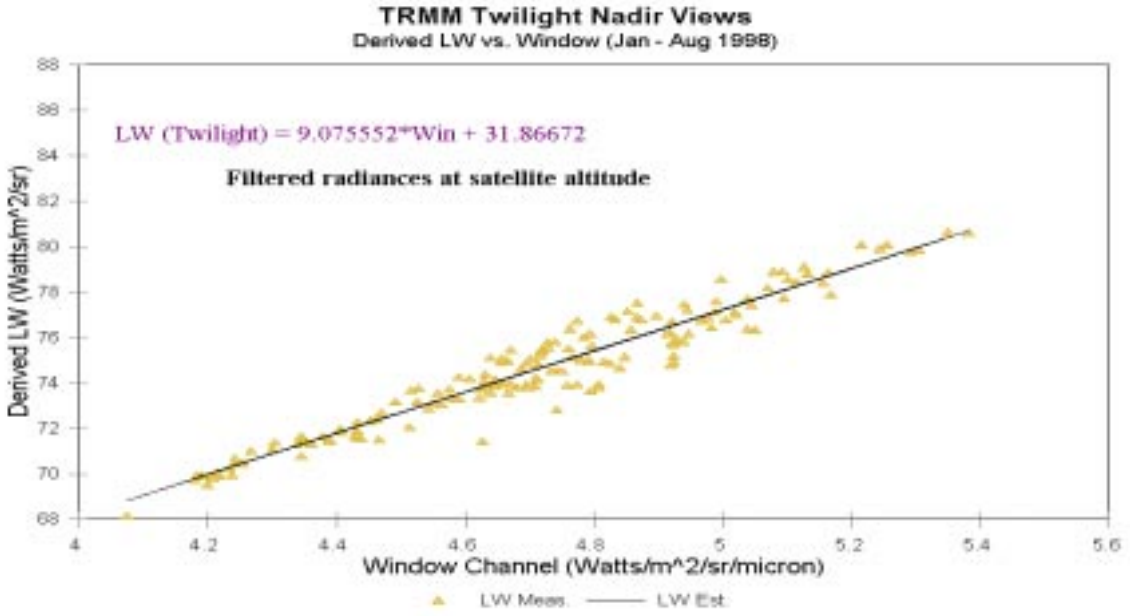

Figure 12. Twilight: Estimated LW vs. Window Channel

The various maxima and minima for each data set were examined to determine any distinguishing characteristics between the sets. The shortwave channel measurements easily permit one to distinguish between daytime and either twilight or nighttime data, but it is not possible to distinguish between twilight and nighttime data using the shortwave measurement, because of the overlapping shortwave measurements in both the twilight and the nighttime data sets. Any shortwave measurement greater than 0.48 watts/m^2/steradian is included in the daytime data set; while any shortwave measurement less than 21.79 watts/m^2/steradian is included in either the twilight or the nighttime data sets. In other words, for the data sets which we analyzed, there were no daytime shortwave measurements less than 21.79 watts/m^2/sr, and no non-daytime shortwave measurements greater than 0.48 watts/m^2/steradian. The problem of determining which regression equation to use ultimately rests on the magnitude of the shortwave measurement for the sample, which is directly dependent on the SZA. As an additional step in our analysis, because the differences between the twilight and the nighttime data sets was not readily apparent, we created a fourth data set by combining the twilight and nighttime data sets into what we call the non-daytime set. A linear regression was performed on this data set.

Figure 13 displays the results of the regression. It is important to note that the data depicted in Figure 13 represents data for which the SZA was greater than 90°.

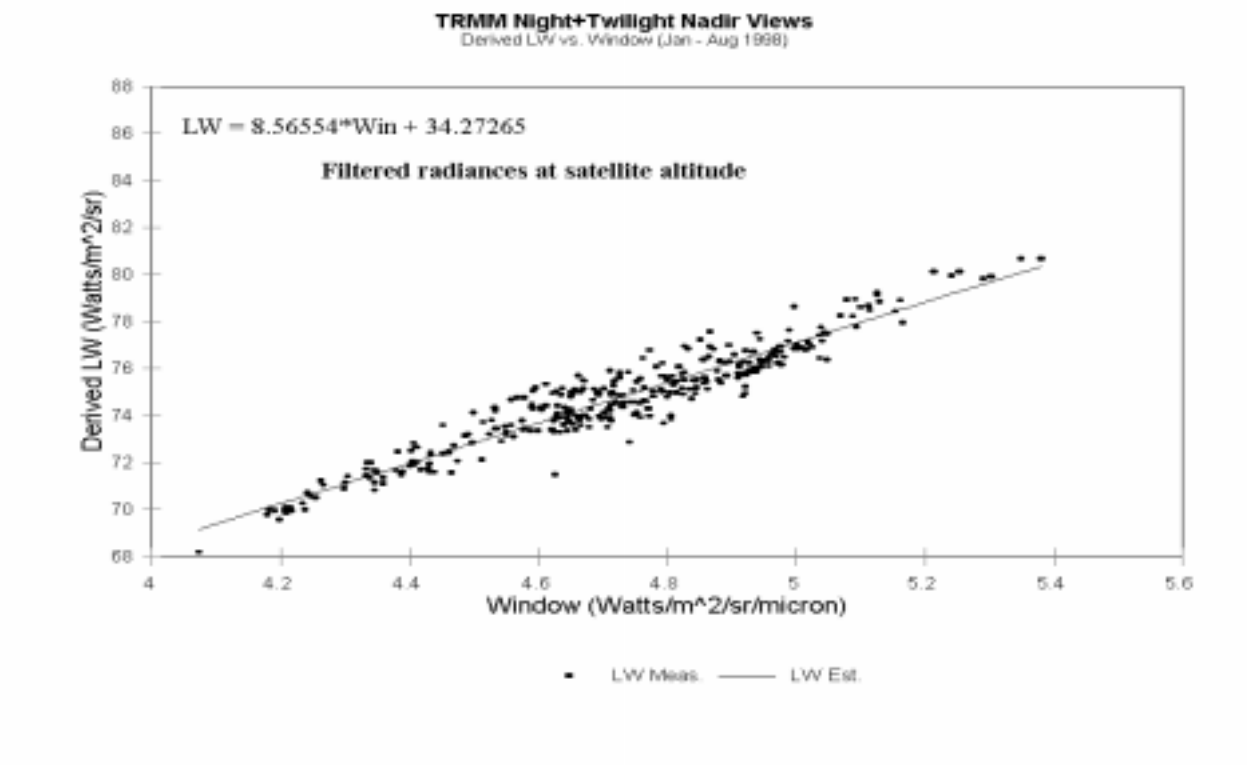

Figure 13. Non-daytime: Estimated LW vs. Window Channel

Although it is a very "busy" graph, the combined results of regressions for all four of the data sets shown above are shown in Figure 14, where we have written the boolean terms for the composite (nighttime + twilight) dataset as functions of the SZA rather than the shortwave measurement. The SZA is being used because it is, in all respects, a

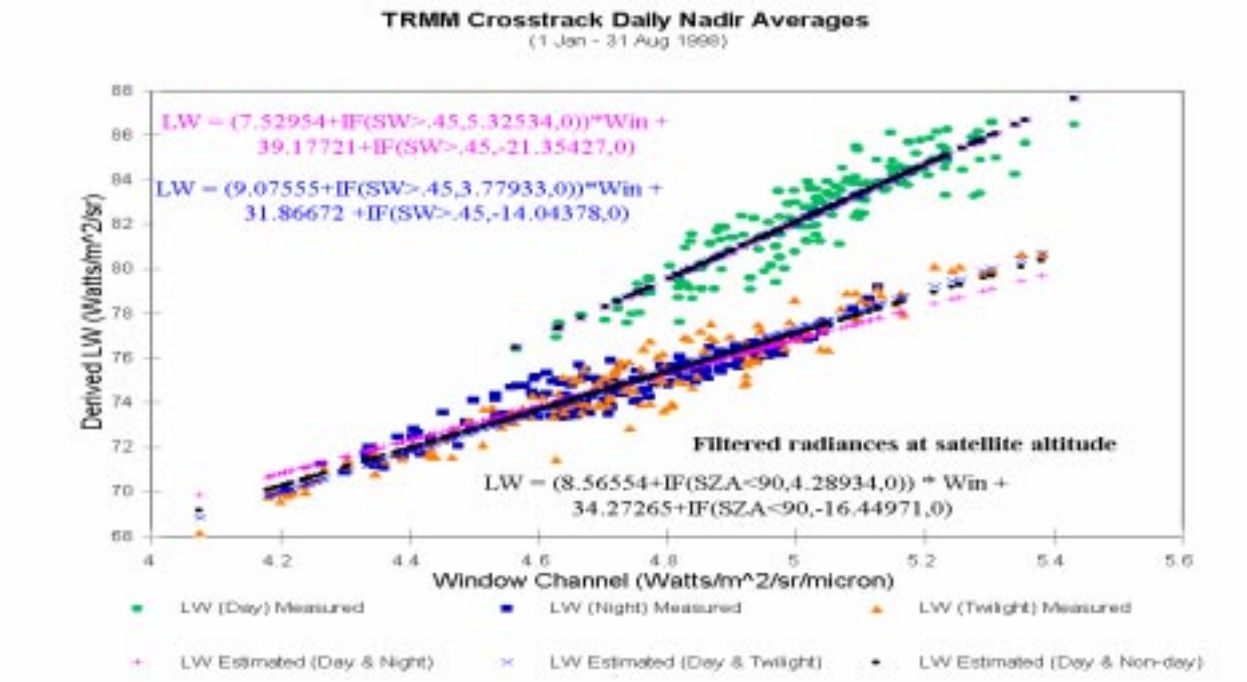

Figure 14. Measured and regressed values for all data sets

measurement which can be used in lieu of a shortwave measurement to resolve the daytime/nighttime question. The regressed values for all of the measured data points are shown in the plot as the symbols which appear to be aligned. The gain terms for the nighttime, non-daytime (or composite), and twilight data sets are not widely different, being 7.529537, 8.56554, and 9.075552 respectively. The daytime data set is the only truly distinct set, as its gain term (12.85488) clearly differs from the gain terms for the twilight, nighttime, and non-daytime data sets. The fact that there is little difference between the twilight and the nighttime data sets is not surprising, because the data sets we are using for this paper are restricted to the nadir-views. Hence, with an SZA > 90° one has every reason to expect that the scene will be in total darkness except for some slight atmospheric refraction effects at, or very close to, the terminator. We have defined the "error" of the regressed values to be the percentage ratio of the standard deviation of the measurements from the mean at each point to the mean regressed value. Using this definition, we obtained the error estimates summarized below in Table 1.

Table 1: Estimated Averaged Errors in LW Regressions

Data sets included	Estimated averaged error
Daytime & Nighttime	1.04%
Daytime & Twilight	1.01%
Daytime & Non-daytime	1.00%

6. CONCLUSIONS

By combining the regression equations for the various data sets just described, we derived an equation, with boolean terms, which described the means of all of the data sets for all conditions. Our analysis shows that by using this equation, and any two CERES radiance measurements, we can predict the longwave component to within approximately 1% of its true value. We believe that this is an important validation result, for it means that the failure of any one of the three sensors (i.e., total, window, or shortwave) in the CERES instrument will be immediately obvious from the solar zenith angle of the instrument and the measurements taken by the remaining two channels. Moreover, it is possible to do this without using any modeling tools (e.g., unfiltering or inversion,) or data measurements from an independent source.

7. ACKNOWLEDGEMENTS

We would like to thank Jim Kibler and Chris Currey of the Data Management Office, Atmospheric Sciences Competency, NASA/Langley Research Center. Jim for suggesting that we take a hard look at the data for the different modes of operation; and Chris for providing the nadir-view subset files of the CERES/TRMM data used in this paper, without which this analysis would have been a much more difficult task.

8. REFERENCES

1. B. R. Barkstrom, "Earth radiation budget measurements: pre-ERBE, ERBE, and CERES," in *Long-term Monitoring of the Earth's Radiation Budget*, B. R. Barkstrom, ed. **Proc. Soc. Photo-Opt. Instrum. Eng., 1299,** 52-60 (1990).

2. B. A. Wielicki, B. R. Barkstrom, E. F. Harrison, R. B. Lee III, G. L. Smith, and J. E. Cooper, "Clouds and the Earth's Radiant Energy System (CERES): and Earth Observing System Experiment," **Bul. Amer. Met. Soc., 77,** 853-868 (1996)

3. R. B. Lee III, B. R. Barkstrom, G. Louis Smith, J. H. Cooper, L. P. Kopia, and R. W. Lawrence, "The Clouds and the Earth's Radiant Energy System (CERES) Sensors and Preflight Calibration Plans," **Journal of Atmospheric and Oceanic Technology, 13,** 300-313 (1996)

4. J. J. Chapman, J. Bockman, V. M. Clark, P. C. Hess, and M. S. Grant, "Assessment of selected CERES electronic component survivability under simulated over-voltage conditions," **Proc. Soc. Photo-Opt. Instrum. Eng., 3750,** (in-press, paper 3750-63, 1999.)

Further author information:
J.P.(correspondence): email: j.paden@larc.nasa.gov; WWW: http://earth-www.larc.nasa.gov/~jack/;
Telephone: 757-827-4880; Fax: 757-825-9129
D.K.P.: email: d.k.pandey@larc.nasa.gov; Telephone: 757-827-4890; Fax: 757-825-9129
R.B.L.: email: r.b.lee@larc.nasa.gov; Telephone: 757-864-5679; Fax: 757-864-7996
K.J.P.: email: k.j.priestley@larc.nasa.gov; Telephone: 757-864-8147p; Fax: 757-864-7996